© *Proc.Indian natn. Sci. Acad.*, **52**, A, No. 1, 1986, pp. 338–362
Printed in India

PROTON CONDUCTION IN SOLIDS*

S CHANDRA, N SINGH** *and* S A HASHMI

Department of Physics, Banaras Hindu University, Varanasi-221005, India

(*Received 4 December 1985*)

Recent advances in the study of solids with high proton conductivity have been reviewed. Many superionic solids or solid electrolytes have been developed for Ag^+, Cu^+, Li^+, Na^+, K^+, F^-, O^{2-} but not many good proton conducting solids are still available. Reasons for this have been identified. Important experimental techniques for studying proton transport have been outlined. Two novel techniques for the study of ion transport used by us are laser Raman and NMR studies under d.c. bias. A general discussion of different transport mechanisms is also presented.

Solid hydrates have been identified as a special group of materials which can sustain high proton conduction. Recent investigations in our laboratory have shown that the interlayer water or water of crystallization of these solid hydrates can be electrolysed which supply the mobile charge carriers.

Applications of solid proton conductors are also reviewed. Special mention has been made of two devices studied in our laboratory, viz. solid state dehumidifier and *in situ* solar energy storage system.

Key Words: Proton Conduction and Conductivity; Superionic Solids; Ion Transport; Laser Raman, IR and NMR Spectra; D.C. Bias; Solar Energy Storage System

INTRODUCTION

THE charge transport in solids takes place *via* : (*i*) electrons (*ii*) holes and (*iii*) positive and negative ions. Electrons are the charge carriers in metals. In semiconductors, the conductivity can be due to electrons and/or holes. Alkali and silver halides are the earlier known solids in which conductivity is due to ion motion. Their ionic conductivity was, however, very small ($\sim 10^{-14} - 10^{-16}$ ohm^{-1} cm^{-1}). Recently, a large number of solids discovered show high ionic conductivity.[1] Such solids termed as fast ion conductors or solid electrolyte or superionic solids, conduct monovalent cations (e.g. H^+, Li^+, Na^+, K^+, Ag^+, Cu^+) with the exception of anion conductors for O^{2-} and F^-. For high conductivity, the number of charge carriers as well as their mobility should be large. The ion transport may be facilitated by the thermally generated point defects or may be provided by some inherent structural disorder. This review tries to present an overview of the perspectives and problems associated with fast proton transport in solids. The proton conductors are of great use in fuel

*Based on the Talk delivered in the INSA-Golden Jubilee Symposium on Solid State Chemistry held at INSA, New Delhi during December 4-6, 1985.

***Present Address** : Gaya College, Magadh University, Gaya.

cell, hydrolysis cell, high energy density batteries and charge transport in complex biophysical system. However, no reliable work was started until a few years ago despite many earlier claims of proton conduction in a series of solids.[2]

Mechanism of Ion Transport–Phenomenological and Structural Approach

The ionic solids can broadly be grouped into the following two groups on the basis of their conductivity or defect structure :

i. Point defect type Insultating Ionic Solids, and

ii. Molten Sublattice type Superionic Solids.

The transport mechanism for the two types are entirely different as briefly described below.

Transport in Point Defect Type Ionic Solids

The ionic solids belonging to this class (viz., alkali and silver halides) possess conductivities lower than 10^{-10} ohm^{-1} cm^{-1} at room temperature.

An ideally perfect ionic crystal would be an insulator if the ion transport under the action of an electric field is assumed to take place *via* anion-cation exchange only. This process involves a very high energy of $\sim$ 15eV.[3] However, all ionic solids are known to have a finite (though small) conductivity. This is attributed to the presence of thermally generated Schottky and Frenkel defects in the lattice. These 'point defect type' ionic solids can be further sub-divided according to the defect concentration as follows :

(a) Dilute or low concentration

The number of mobile defects is $\leqslant 10^{18}$ cm^{-3}.

Examples are (alkali and silver halides).

(b) High concentration

The defect concentration is $> 10^{18}$ cm^{-3}.

These solids behave as fast ion conductors at high temperatures. Examples are (Stabilized Zirconia or Hafnia, CaF_2 etc.)

In general, the electrical conductivity is given by :

$$\sigma = \sum_i n_i q_i \mu_i, \qquad \ldots(1)$$

where, n_i is the number of charge carrier, q_i the charge on the ith ion, and μ_i the mobility of the charge carrier or ith ion.

Here, the charge carriers are thermally generated Frenkel or Schottky defect pairs. Their number (n_i) and mobility (and hence the conductivity) are temperature dependent.[3] The number of these Frenkel (n_F) and Schottky (n_S) defects are given by the following expressions :

$$n_F = (NN')^{1/2} \exp\left(-\frac{g_F}{2KT}\right); \qquad \ldots(2)$$

and

$$n_S = N \exp\left(-\frac{g_S}{2KT}\right), \qquad \ldots(3)$$

where g_F and g_S are the energies of formation of Frenkel and Schottky defects. N' is the number of normal lattice sites per unit volume. N' is the number of interstitial sites per unit volume.

The ionic mobility μ_i is given by the expression

$$\mu_i = \frac{a^2 q_i}{KT} \nu_0 \exp\left(\frac{-\Delta G}{KT}\right), \qquad \ldots(4)$$

where ν_0 is the vibrational frequency of the ion around its equilibrium position,

ΔG is the energy difference between the saddle point and lattice site position (i.e., energy barrier for the migration of ion)

and a is the interatomic distance.

Hence, the conductivity for materials with Schottky or Frenkel defects is given by

$$\sigma_S = n_S \mu_S q = \frac{Na^2 q^2 \nu_0}{kT} \exp\left(-\frac{g_S/2 + \Delta G_S}{kT}\right) \qquad \ldots(5)$$

and

$$\sigma_F = n_F \mu_F q = \frac{(NN')^{1/2} a^2 q^2}{kT} \nu_0 \exp\left(-\frac{g_F/2 + \Delta G_F}{kT}\right). \qquad \ldots(6)$$

It is obvious that a plot between $\log \sigma T$ *vs* $1/T$ would be linear for both the cases.

In the above discussion, we have assumed that all the defect pairs are thermally generated. However, doping can also change the defect concentration (and hence the conductivity). For detailed analysis of doped alkali halides reference may be made to Chandra and Rolfe[4], Fuller[5], Friauf[6] and Chandra.[1]

The defect concentration, in general, can be altered by aliovalent doping apart from changing the temperature. For most cases the conductivity of ionic conductor is due to both the above reasons. So, 'point defect type' superionic conductors generally show high conductivity only at high temperatures. For example, PbF_2 is a good fluorine ion conductor at high temperatures only because of the increased number of thermally generated Frenkel interstitials.[7] The O^{2-} ion conductors are doped ZrO_2, HfO_3, ThO_2, CeO_2 etc, in which tetravalent cations are partially replaced by di or trivalent impurities (Ca^{++}, Y^{+++} etc).

Transport in Molten Sublattice Type Superionic Solids

A disordered or defect structure provides a situation where mobile ions are possible. One way is to create this by generating point defects thermally or through doping as described above. The other more promising situation is an inherently

disordered structure where the available mumber of sites in one or both the sublattices are more than the ions, permitting ions to 'hop' almost like a 'free ion' from one site to another. All these ions act as charge carriers. The high mobility or conductivity in this class of solids is further permitted by a 'channelled' or 'layered' structure. The number of mobile ions are $\sim 10^{22}$ cm^{-3}. The study of fast ion transport in a large number of materials indicates several, more or less, common criteria for high ionic mobility as given below.

(i) *Ionic Radii and Charge*—A small cation or anion is likely to move more freely than a relatively large ion in a lattice. The cations have relatively small ionic radii compared to anions. Therefore, most of the superionic materials developed so far are for monovalent cations like Li^+ (0.60Å), Na^+ (0.95Å), K^+ (1.33Å), Cu^+ (0.96Å) and Ag^+ (1.13Å). The anions have large ionic radii, e.g. F^- (1.36Å) and O^{2-} (1.40Å) and so anionic conductors are difficult to obtain at low temperatures. Recently, Dunn and Farrington[8] have reported a few materials showing high mobility at high temperatures for divalent cation Ba^{2+}, Cd^{2+}, Sr^{2+} though it is much less than that for monovalent ions. This is somewhat expected since the coulombic energies involved in jumping/hopping of di-or-trivalent ions are more than that for monovalent ions.

Another related criterion is that the mobile ions should be weakly bound to the rigid lattice. Smaller ions are called upon to be bonded more strongly to the lattice, whereas the small ionic radii would permit greater ease in its movement as discussed earlier. Therefore, in most materials a compromise has to be struck between both these effects which control the net mobility. For example, Li^+ ion in Li-β alumina despite its small ionic radii or size, is much less mobile than Na^+ in Na-β alumina, apparently as a consequence of a weaker Na-0 bond.[9]

(ii) *Ionic Polarisability*—Diffusion through the faces of the coordination polyhedron is made easier by the large polarisability of the mobile species as well as that of antagonist ion. The latter possibly distorts its electronic cloud during movement of the mobile ion. Analysis of the electronic properties of various fluorides crystallizing with the same structure shows that larger is the polarisability of the cations, the greater is the ionic conductivity.[10]

(iii) *Covalency of rigid lattice*—Ionic mobility would be higher if the bonding energy between the mobile ion and antagonist ion is weak. A good example is LaF_3 which involves three types of fluorine atoms. The more mobile anions have the longest La-F distance.[11] Another interesting example is that of ternary compounds of formula $MM'_m X_n$, in which the M-X bond may be weakened as a consequence of a strengthening in the competing M'-X bond. Consequently, in isostructural materials, the optimal mobility is obtained when the rigid lattice is the most covalent possible. Such examples are hollandite type materials.[12–14]

(iv) *Coordination Number of Mobile Species*—Fast ionic mobility is easier for mobile species with low coordination number because a large opening of the 'bottle neck' is provided between the two neighbouring sites. In some Ag^+ and Cu^+ good ionic conductors the mobile cations have coordination numbers 4,3,2 in the

equilibrium positions[15] whereas silver is 6-coordinated in poor ionic conductors like AgF, AgCl, AgBr.

Similarly for anionic conductor the lower is the coordination number of anion, the greater is its mobility.[10] For example, in NaF, CaF_2 and LaF_3 the fluorine anionic coordinations are 6, 4 and 3 respectively and consequently their conductivities are such that $\sigma_{NaF} < \sigma_{CaF_2} < \sigma_{LaF_3}$.

(v) *Structure and Concentration of Mobile Ion*—For a large concentration of mobile ions, the energy difference of the cation-anion interaction in the various sites involved in the conduction mechanism should be small. Further, there must be a sufficient number of vacant sites for an ion to hop/jump. Structure is probably the most important factor responsible for high ionic conduction. Table I gives the structural parameters of some superionic solids. A highly 'disordered structure' is the common factor in all the materials which means that the number of sites in the cationic sublattice is more than the number of cations in the unit cell. Thus the percentage occupancy of each site is low. A free ion like hopping of these ions from one site to another may take place giving high conduction. One typical example is α-AgI where the number of sites per unit cell is 12 as against the number of ions which is 2. So the $2Ag^+$ ions can jump freely into the 12 sites available in that unit

TABLE I

Structural parameters of some superionic solids

Material	Structure	No. of cation sites/unit cell	No. of cations/ unit cell	Reference
α-AgI	b.c.c. $a = 5.06$ A	12	2	Wiedersich and Geller[16]
$RbAg_4I_5$	Cubic $a = 11.24$ A	56	16	Wiedersich and Geller[16] (Isomorphus-KAg_4I_5 and $NH_4Ag_4I_5$)
$[(CH_3)_4N]_3A_{13}I_{15}$	Hexagonal $a = 12.77$ A, $c = 26.54$ A	123	39	Geller and Lind[17]
$(C_5H_5NH)\ Ag_5I_6$	Hexagonal $a = 11.97$ A, $c = 7.41$ A	34	10	Geller[18] Geller and Owens[19]
α-Ag_3SI	b.c.c. (disordered)	12	3	Wiedersich and Geller[16]
$Ag_7I_4PO_4$	Cubic $a = 10.6$ A	—	—	Takahashi *et al.*[20]
$(C_5H_5NH)_2Cu_5Br_7$	Space group $P_{2_12_12_1}$ $a = 13.09$ A, $b = 14.04$ A $c = 11.78$ A	52	20	Chan and Geller[21]
Li_2SO_4	f.c.c. $a = 7.07$ A at 610 °C	3	2	Forland and Krogh-Moe[22]
Li_4SiO_4	Monoclinic	18	8	Vollenkle *et al.*[23]

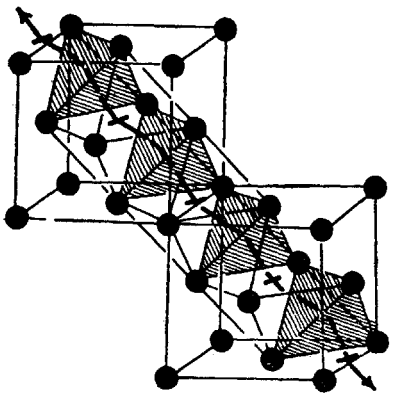

FIG 1 An almost linear passage way in an fcc anion lattice.

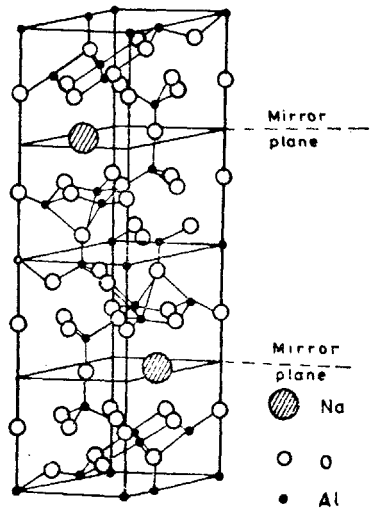

FIG 2 Crystal structure of β-alumina primitive unit cell.

cell. For mobility between cells a face shared polyhedra provides the channelled structure given in Fig. 1. Another interesting example is that of β-alumina (Fig. 2) where the low percentage occupancy for each site is also present. β-alumina has a layered structure in which there are three categories of cationic sites referred to as B-R, *a*-Br sites, mid oxygen (m.o) sites[24] possessing different percentage occupancies.

SPECIAL PROBLEMS OF PROTON TRANSPORT

As discussed above, two important criteria for high ionic conductivity are that the moving ion must be monovalent with small ionic radii. Both these criteria are satisfied for H^+ion, yet there are not many good proton conductors available. Some of the special problems of proton conduction are listed below.[25]

(i) Naked H^+ ions are not found in solids under equilibrium condition ($\tau > 10^{-11}$ sec). H^+ is always covalently bonded to some electronegative atoms/ions in the structure e.g. C–H, N–H, O–H.

(ii) Protons can be shared between two electronegative atoms e.g., O–H–O. This is the so-called hydrogen bond.

(iii) Oscillation of H from one side to the other in a hydrogen bond O–H–O⇌ O–H–O corresponds to a net transport of charge and is, therefore, an essential step in the proton conduction mechanism.

(iv) Proton conduction differs from the conduction of other ions (Na^+, K^+, Ag^+) principally in the following ways :

(*a*) Hydrogen bond is covalent and directional in character, whereas metal ions in ionic solids experience coulomb forces more or less from all sides.

(*b*) As a consequence, proton conduction involves at least two different steps as opposed to one step process for the other metal ion conduction.

Different suggested transport mechanisms for proton conduction in solids are :—

(*i*) *Liquid-like Transport*

Liquid-like transport is possible in : (*a*) materials which contain water layers included in the crystal structure such as H-montomorillonite, H-Al-Montmorillonite and H-Al-Fe-montmorillonite clay.[26] In these materials (clays) interlayer water forms liquid-like network permitting high protonic conductivity due to the liquid-like motion of H^+. (*b*) Polycrystalline materials composed of charged crystallites held together by an electrolyte solution.

(*ii*) *Proton Jump followed by Reorientation*

This mechanism will function with the following acid/base couples properly located at alternating positions

$$H_3O^+/H_2O,\ NH_4^+/NH_3,\ R\text{-}COOH/RCOO^-$$

$$H_2O/OH^-,\ R\text{-}NH_3^+/R\text{-}NH_2,\ RSO_3H/RSO_3^-$$

$$OH^-/O^{--}.$$

The proton jump is possible by tunnelling in a hydrogen bond. The mechanism involves two steps as follows:—

(*i*) In the first step the proton is transported by tunnelling (or hopping) in hydrogen bond (e.g., $H_3O^+ \rightarrow H_2O$; $NH_4^+ \rightarrow NH_3$ etc.).

(*ii*) In the second step, the subsequent reorientation of neutral molecules (e.g. H_2O, NH_3.....) thus formed to occupy the vacant proton positions.

The molecular reorientation during proton conduction is shown in Fig. 3 as an example for hydrogen uranyl phosphate ($HUO_2\ PO_4.4H_2O$). In this material, which is 'acidic hydrate', alternating layers of UO_2^+ and PO_4^{3-} ions contain layers of H_2O

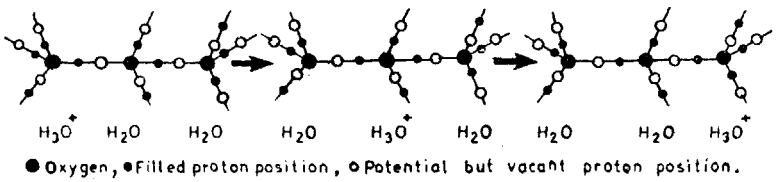

FIG 3 Illustrative example of proton motion in $HUO_2PO_4.4H_2O$.

and H_3O^+ ion. The ratio of H_3O^+ to H_2O is 1 to 3 where hydrogen bonding is dominating. Other examples of acid hydrate group are $HUO_2.AsO_4.4H_2O$, $H_3PW_{12}O_{40}.29H_2O$ and $H_3PMo_{12}O_{40}.29H_2O$,[28] $H_3O,Al_3(SO_4)_2(OH)_6$,[29] $H_8UO_2(IO_6)_2.4H_2O$,[30] H_3O^+-β-alumina etc.[31]

Another example is that of a basic hydrate $[Zn_2Cr(OH)_6]$ OH nH_2O[32] which shows conduction due to proton exchange between H_2O and OH^- species. Here in the positively charged layers of $[Zn_2Cr(OH)_6]^+$, the interlayer of $[X\text{-}nH_2O]^-$ are present, $[X^- = OH^-]$. Similar is the case for other acid/base groups. The transport phenomena is known as 'Grotthus type mechanism.' The activation energy lies entirely in the reorientation step. Thus, net activation energy is low.

(iii) Polyatomic Ion Transport

This type of conduction prevails in compounds, where the corresponding acid/base partners are not present i.e., H_3O^+ without excess H_2O, OH^- without O^{2-} or H_2O; and NH_4^+without NH_3 are present in the material. The polyatomic ions H_3O^+, OH^- or NH_4^+ migrate as entities through the bulk material. The activation energy is expected to be very high. This is known as 'vehicle mechanism.[33] In solids like $LiN_2H_5SO_4$,[34] H_3O^+-β-alumina and NH_4^+-β-alumina,[35] NH_4^+-Zeolite,[36] $H_3O\ UO_2\ AsO_4\ .3H_2O$[37] polyatomic species like H_2O^+, $N_2H_5^+$, NH_4^+ etc. migrate as entities on application of electric field.

The 'vehicle mechanism' and 'Grotthus mechanism' are pictorially illustrated in Fig 4.

MATERIALS

The various protonic conductors can be classified as:—[1,2]

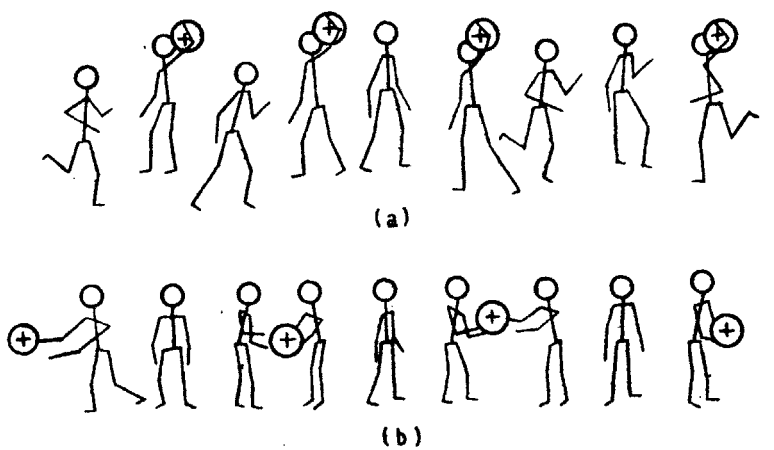

FIG 4 (*a*) Polyatomic ion transport or "Vehicle mechanism."
(*b*) Co-operative ion motion (with reorientation + hopping) or Grotthus mechanism.

A. Non-Hydrogen-Bonded Systems

(*i*) Materials lacking stoichiometric hydrogen in which proton occurs either by defect equilibria with water and/or hydrogen or secondly by electrical injection of protons from adjacent layers. A few metal oxides like Cu_2O, CoO, NiO, ZnO, TiO_2 etc. may sustain protons $\sim 10^{-5} - 10^{-7}$ mole fraction.

(*ii*) Aromatic hydrocarbons without hydrogen bonds are also possible candidates for proton conduction. However, not many compounds have been reported. Anthracence probably has some protonic conduction.

B. Hydrogen-Bonded Systems

(*i*) Isolated hydrogen bonds in small carboxylic acids; hydroxy compounds (orthoboric acid H_3BO_3, pentaerythyritol etc.); alkali metal fluorides (like KHF_2) allow some proton conduction.

(*ii*) A large group of materials with chains of hydrogen bonds broken by intramolecular links have been found to show proton conduction like NH_4Cl, $(NH_4)_2$ So_4, ammonium perchlorate, oxonium perchlorate, triglycine sulfate (TGS), the KDP ferroelectric family, amino acids, a few hydrates, borax, imidazole etc.

(*iii*) A few materials with linked chains of hydrogen bonds also show protonic conduction like ice, alcohols etc.

C. Organic Polymeric Systems

Polyamides (nylon), polysulphinimide $(SONH)_n$, mylar etc., are some familiar examples.

D. Biological Systems, Including Biopolymers

Some of the proton conductors are listed in Table II.

Some Experimental Results

We wish to discuss some unusual results recently obtained by us on two hydrates viz. Molybdic acid, $MoO_3.2H_2O$ and Ammonium para-tungstate $(NH_4)_{10}$. W_{12}-$O_{41}.5H_2O$. Glasser[2] has identified some important experimental techniques necessary for the study of proton conductors. A major problem in the field of proton conductor is a definite proof that charge transfer in the solid occurs by motion of protons. Some of the techniques used are:—

- Time-dependent polarisation (including Maxwell-Wagner dispersion
- Coulometric measurement
- Space-charge Polarisation
- Electrical conductivity and thermoelectric power
- Diffusion
- Ion Dynamics by NMR, IR, Raman, Electron paramagnetic resonance, Neutron scattering etc.

TABLE II

Materials	Sp. Conductivity (ohm^{-1} cm^{-1}) at room temp.	Proton Conduction Mechanism
(i)	(ii)	(iii)
1. $HUO_2PO_4.4H_2O$ (HUP)	4×10^{-3}	H_3O^+/H_2O jump
2. $HUO_2ASO_4.4H_2O$ (HUAs)	6×10^{-3}	H_3O^+/H_2O jump
3. $H_8UO_2(IO_6)_2.4H_2O$	7×10^{-3}	
4. $Sb_2O_5.nH_2O$	3×10^{-4}	H_3O^+/H_2O jump
5. $(H_3O)\ Al_3(SO_4)_2(OH)_6$	3×10^{-4}	H_3O^+/H_2O
6. $Sb_2O_5.4H_2O$	10^{-3}	H_3O^+/H_2O jump
7. $[H(H_2O)_n]_{12}Sb_{12}O_{36}$	10^{-7}	H_3O^+/H_2O jump
8. $H_3OUO_2ASO_4.3H_2O$	—	H_3O^+/H_2O at high pressure H_3O^+ migration at low pressure
9. $[Zn_2Cr(OH)_6]OH.nH_2O$	6×10^{-4}	H_2O/OH^-
10. β-KOH (248 °C)	10^{-3}	H_2O/OH^-
11. $H_3PMo_{12}O_{40}.29H_2O$ (PMA)	1.8×10^{-1}	Liquid like transport of H^+
12. $H_3PW_{12}O_{40}.29H_2O$ (PWA)	1.7×10^{-1}	Liquid like transport of H^+
13. H^+ montmorillonite clay	1.4×10^{-4}	Liquid like transport of H^+
14. H-Al montmorillonite clay	10^{-4}–10^{-2}	Liquid like transport of H^+
15. $MoO_3.2H_2O$	10^{-5}	Liquid like electrolysis
16. $In(OH)_3.4H_2O$	10^{-3}	Liquid like transport of H^+
17. $(NH_4)_{10}W_{12}O_{41}.5H_2O$	10^{-6}	—
18. $Al(OH)_3.4H_2O$	6×10^{-8}	Liquid like transport of H^+
19. $Ca_2O_3.4H_2O$	10^{-4}	Liquid like transport of H^+
20. $SnO_2.3H_2O$	2×10^{-4}	Liquid like transport of H^+
21. $ZrO_2.23H_2O$	3×10^{-5}	Liquid like transport of H^+
22. $H_3O.ClO_4$	3×10^{-4}	H_3O^+ migration of impurity conduction
23. Hydrated hydronium β-alumina	5×10^{-3}	H_3O^+/H_2O jump H_3O^+ migration
24. NH_4^+-β-alumina	10^{-3}	NH_4^+ migration
25. NH_4^+-zeolite	2×10^{-3}	NH_4^+ migration
26. $LiN_2H_5SO_4$	2×10^{-8}	N_2H_5 migration
27. $SnCl_2 2H_2O$	10^{-6}	Liquid like transport
28. $(NH_4)_3H(SO_4)_2$	10^{-3}	—
29. LiH_2PO_4	10^{-3}	$R\text{-}PO_3H/R\text{-}PO_3^-$
30. $SrCe_{1-x}M_xO_3$ (600 °C) (M = Y, Yb, In, Zn, Nd)	10^{-3}	Conduction by electron holes
31. $N_2H_6SO_4$ (200 °C)	10^{-4}	Reorientation followed by hop

It must be, hower, noted that no single technique would be able to tell unambiguously about the proton transport. A combination of many techniques may reasonably decide the transport mechanism. Some of the more common techniques are :

(*a*) *Coulometric Measurement*

When current is passed between electrodes holding the sample, the electrochemical product of the conduction in the form of gas at the negative electrode is

collected and measured. The percentage of charge carried by the protons can be calculated from the volume (and hence the mass) of gas collected.

(*b*) *Nuclear Magnetic Resonance*

The dynamics of proton motion in solids is best studied by NMR. A 'line-narrowing' occurs when the proton is free to move. Further, the relaxation time measurements also help in knowing the detailed ion dynamics.

(*c*) *IR and Raman Spectra*

The presence of low frequency modes in laser Raman spectra are generally indicative of a free-ion situation. Sometimes, the IR spectrum is also found to be broadened and modified as a result of proton-tunneling or weakening of hydrogen bond. Chandra and Singh[38] tried to locate the mobile H^+ by looking at the IR spectra of original sample and a sample from which some protons have been transported out by electrolysis during coulometric experiment.

(*d*) *Neutron Scattering*

Diffuse X-ray and neutron scattering are powerful tools for studying ion dynamics. However, inelastic scattering of slow neutrons is more suited for proton conductors because the incoherent scattering cross-section of hydrogen for neutrons is particularly large.

In the following paragraphs we describe some of the results obtained in our laboratory. The materials fall in the following categories:—

(*i*) *Hydrates*: $MoO_3 . 2H_2O$ and $(NH_4)_{10}\ W_{12}O_{41} . 5H_2O$

(*ii*) *Hydrazine Compounds*: $N_2H_6SO_4$ and $N_2H_6Cl_2$

Coulometry and Transference Number

One of the most difficult problems in proton conductors is to show that actually proton is the mobile species. We developed a direct method in which a specially designed coulometer was used and hydrogen envolved was collected (Fig. 5). While

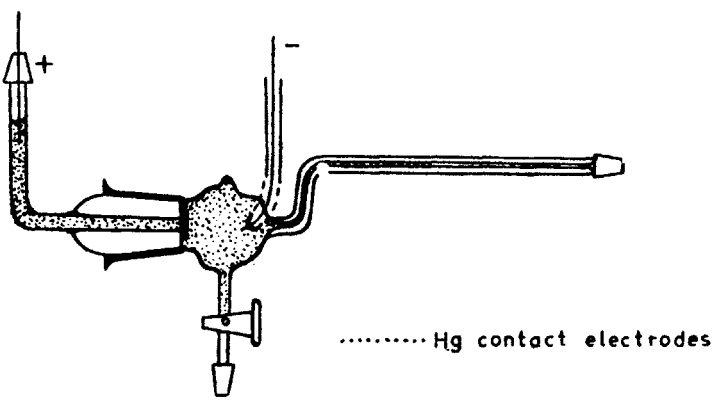

FIG 5 Coulometer.

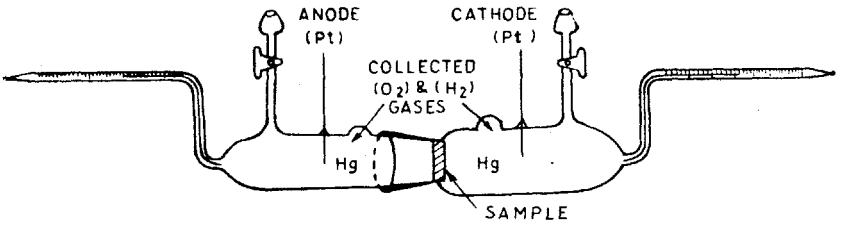

FIG 6 Modified Coulometer or electrolysis cell.

carrying out the experiment on $MoO_3.2H_2O$, we found that the amount of H_2 envolved at cathode is much less than the expected volume from Faraday's law. We suspected that a part of charge is being carried out by O^{2-} produced as a result of electrolysis. Thus, a new hypothesis of possible electrolysis of interlayer water or water of crystallisation was made. To confirm this, a specially designed coulometer or electrolysis cell was used as shown in Fig. 6. The volumes of gases evolved (if any) at cathode/anode could be measured by monitoring the movement of mercury columns in the micro-pipette attached on the two sides. A thin pellet of the sample was mounted by araldite on the cone face separating cathode and anode ends. Electrical contacts at the two faces of the pellets were made with platinum wire electrodes dipped into pure mercury. The electrolysis was carried out at a constant current.

The amount of gases collected (evolved) at the cathode and anode sides of the coulometer are shown in Fig. 7 which have been used for calculating the transference numbers. If the material is essentially an ionic conductor with proton as the only mobile species, one would expect H_2 alone to be collected at the cathode as shown in Fig. 7. The astonishing result is the evolution of O_2 [Fig. 7 (*a*) and 7(*b*)] and Cl_2[Fig. 7(*c*)] at the anode. We propose a new concept that the water of crystallisation is electrolysed in the former cases while HCl is electrolysed in the latter case. We have used IR-studies to confirm our electrolysis hypothesis. The effect of electrolysis is most pronounced in $MoO_3.2H_2O$ where one of the H_2O is interlayer (the other is coordinated) which can be easily electrolysed. For Ammonium paratungstate[39] the protons for the transport are mostly provided by NH_4^+ group while only a small part comes from the electrolysis of H_2O. Similarly, in hydrazine di-hydrochloride, the hydrazonium ion provides most of the protons (as established by Chandra and Singh[38,40] for hydrazine sulphate) and a very small, though finite, part is as a result of electrolysis. The transference numbers for different mobile ionic species in the above studied four compounds are : Molybdic acid ($t_H = 0.69$, $t_{O_2} = 0.18$); ammonium paratungstate ($t_H = 0.79$, $t_{O_2} = 0.14$); hydrazine di-hydrochloride ($t_H = 0.92$, $t_{Cl} = 0.07$); hydrazine sulfate ($t_H = 0.92$).

The transference numbers given above have only limited importance and may actually be in error. When we looked at the sample after the electrolysis experiment was completed, a blackening of the electrode surfaces was noted. This is indicative of some electrode reaction. The possible reactions for $MoO_3.2H_2O$ are as follows :

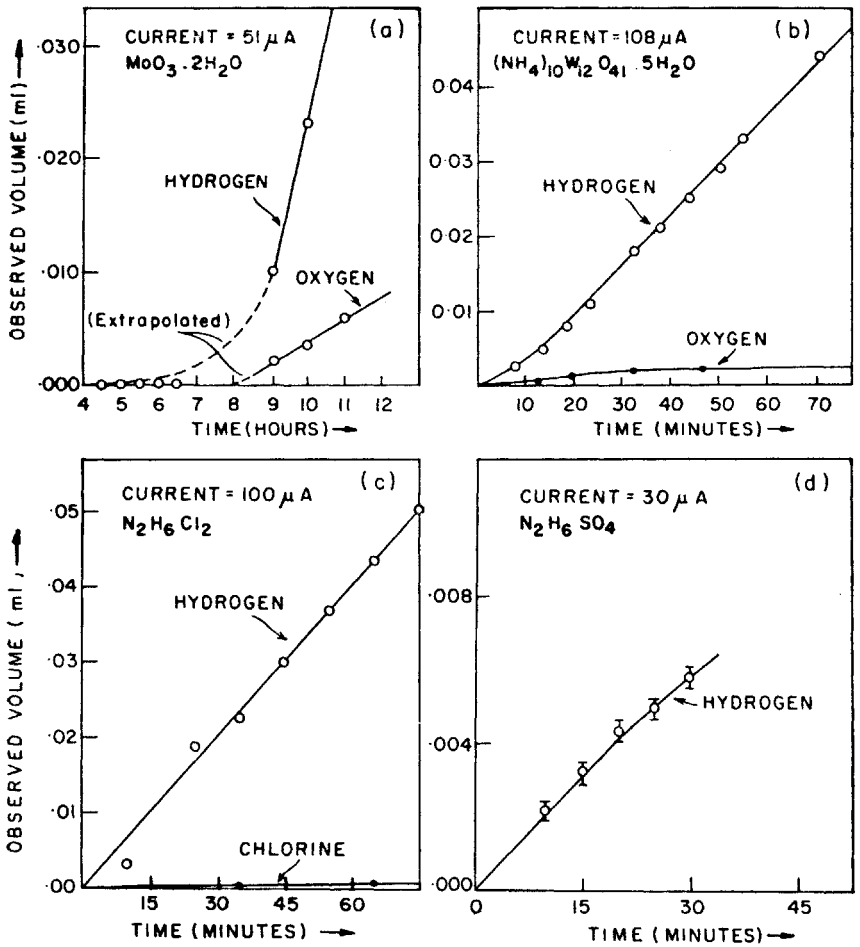

FIG 7 Volume of gases evolved as a function of time.

At cathode $x.H + MoO_3$ (group) $\rightarrow H_xMoO_3$ Bronze (Blue/Grey)

At anode $Hg + 1/2O_2 \rightarrow HgO$

We could not definitely identify the presence of HgO for $MoO_3.2H_2O$ case from IR spectroscopy as the new peak position $\sim$ 1000 cm^{-1} coincided with one of the bands of the monohydrate $MoO_3.H_2O$ (resultant electrolysis product). How ever, this band could be seen in material near the anode surface after the electrolysis of $(NH_4)_{10}\ W_{12}O_{41}.5H_2O$.[39]

Infrared Studies of Electrolysed Sample[39a,b]

In an attempt to identify the hydrogen which has moved out of the sample during electrolysis, we have taken the infrared spectra of electrolysed sample and compared it with the IR spectra of the original sample. These spectra are given in Fig 8. Laser Raman spectra of some of the samples have also been taken and would

be reported elsewhere. The salient features relevant to the present discussion are given below.

The IR spectra of original $MoO_3.2H_2O$ and the material obtained after electrolysis or coulometry experiment are shown in Fig 8(*a*). A comparison of band

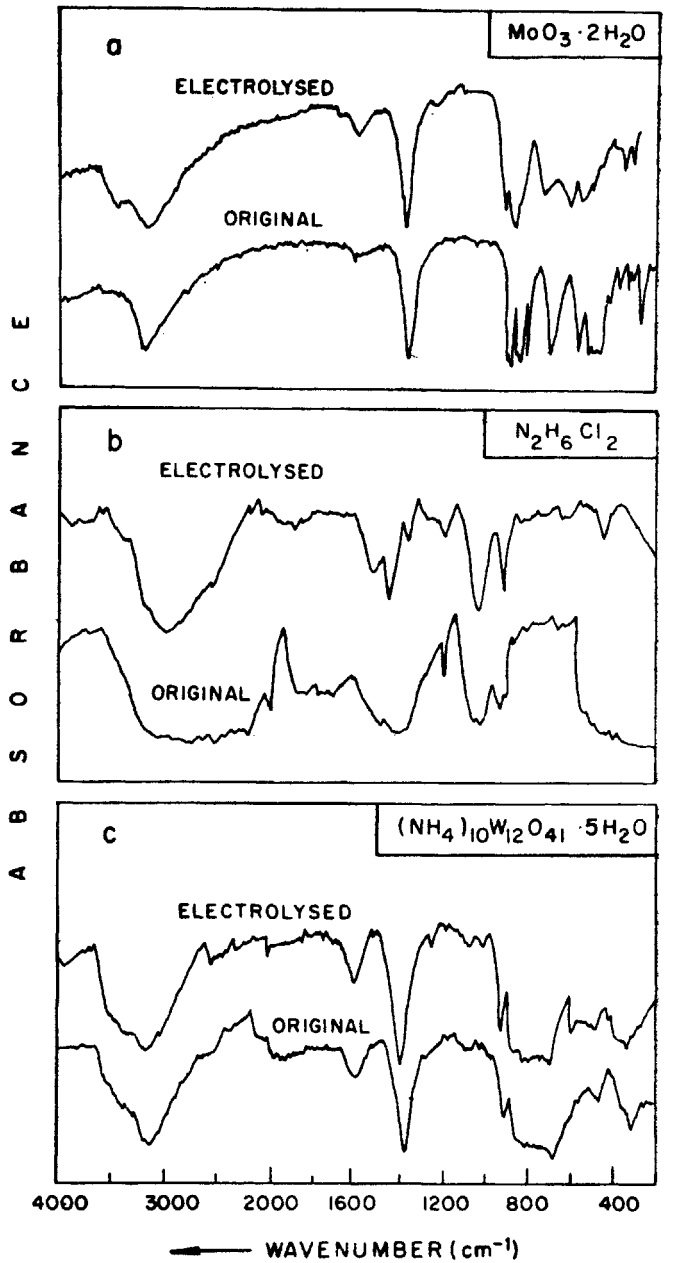

FIG 8 I.R. absorption spectra of the original and electrolysed samples.

positions of these recorded spectra with those already reported in the literature[41–43] shows that the electrolysed material consists of $MoO_3.H_2O$ (monohydrate). This confirms our hypothesis of electrolysis of molybdic acid in which the dihydrate has been converted into monohydrate.

Fig. 8(*c*) gives similar results for ammonium paratungstate. The most distinctive feature is the appearance of two new peaks around 1240 and 3000cm^{-1} in the electrolysed sample. This may be due to lifting of degeneracy as a result of the lowering of symmetry of any particular molecule or ion after electrolysis. We have hypothesized in our coulometry studies on this material that NH_4^+ group provides most of the protons for transport while only a part of it is provided by electrolysis of hydrated water. NH_4^+ ion has T_{dh} symmetry while NH_3 has C_{3v} symmetry. This lowering of symmetry results in one additional bending peak of NH_3 at 1240 cm^{-1} and N-H stretching peak at 3000 cm^{-1}.

Fig. 8 (*b*) gives IR spectra of $N_2H_6Cl_2$ or $N_2H_4.2HCl$. In coulometry we have collected a very small amount of Cl_2 and so most of the hydrogen evolved is not essentially due to electrolysis of HCl group. The IR spectra shows appearance of new peaks at 1400 cm^{-1} and 1235 cm^{-1} and some other features which are characteristics of $N_2H_5^+$ group confirming the removal of a part of hydrogen from $N_2H_6^{++}$ group. Similar results were obtained earlier by Chandra and Singh[38] for hyrazine sulphate.

Laser Raman Spectra under D.C. Bias

Laser Raman spectra (Fig. 9) of the original sample ($MoO_3.2H_2O$) without electrolysis and during electrolysis near cathode and anode separately were recorded at different intervals of time with d.c. bias 'on'. The main differences between the Raman spectra of the original and the electrolysed samples near cathode and anode are given below:—

(*i*) Two new modes appear at 795cm^{-1} and 414cm^{-1}. These bands grow with time of electrolysis as given in Fig. 10. Further, the recorded spectra at the cathode during electrolysis resembles with the reported laser Raman spectra of white or α—MoO_3. H_2O by Saleem and Aruldhas[43] which confirm our earlier IR studies.

(*ii*) The relative intensities of pair of bands, viz. 77cm^{-1} and 88cm^{-1} which are related to translational motion of ions, change. This is more evident in samples near cathode.

(*iii*) The relative intensities of 888cm^{-1} band and water libration mode 846 cm^{-1} also change.

NMR under D.C. Bias

Here, we describe an unusual method for studying ion transport. It is well known that NMR line narrowing occurs in the presence of rotational and/or translational diffusion. Our effort here was to look for the motion of H^+ under d.c. field. To

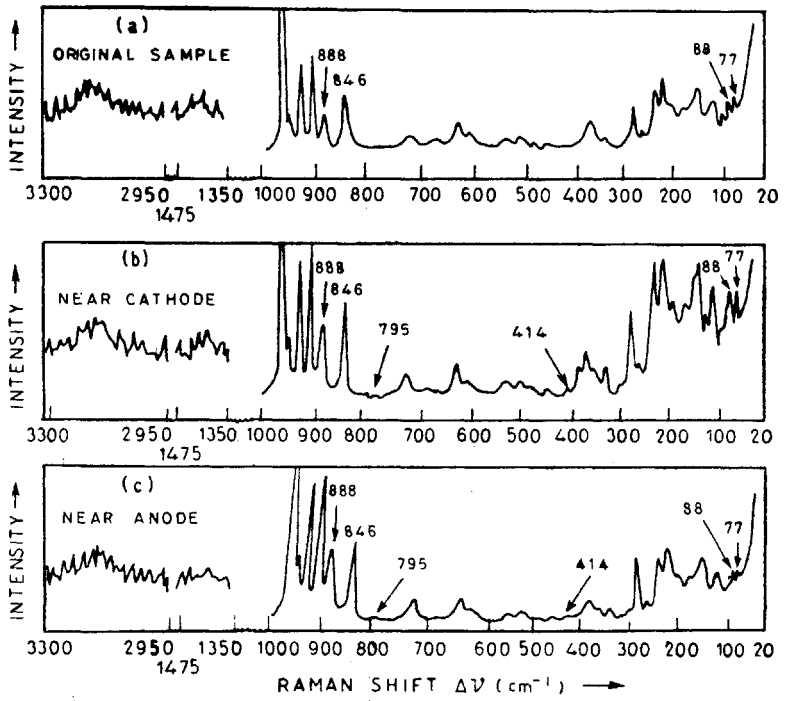

FIG 9 Laser Raman spectra of (*a*) original sample ($MoO_3.2H_2O$) without field, (*b*) sample at cathode when d.c. electrolysis is in progress at 20 volts and (*c*) sample at anode when d.c. electrolysis is in progress at 20 volts.

detect a possible translational diffusion of H^+ we measured NMR line width as a function of applied d.c. bias across the sample. This has been presented earlier by us.[44] NMR line width measurement were made on pressed cylindrical samples of $MoO_3.2H_2O$ placed inside a glass tube. These aquadag silver electrodes were placed on two opposite faces of the pellets. Copper/Silver wire leads were attached to this. ^1H NMR spectra of these samples were recorded at different d.c. bias with the help of a wide line NMR spectrometer at 9.6 MHz. We quote here some of the results reported earlier by us.[45]

The peak to peak linewidths of the recorded derivative signals corresponding to Proton magnetic resonance absorption lines of $MoO_3.2H_2O$ pressed pellets under increasing d.c. bias at different temperatures were measured separately. Following significant observations were noted.

(*i*) At (125 $\pm$ 25) °K the observed derivative signals were found to be highly uniform and symmetric [Fig. 11 (a)]. The measured linewidth was approx. equal to 3.0 Gauss, being independent of increasing d.c. bias at this temperature. This leads us to conclude that at this temperature both water protons behave in similar way.

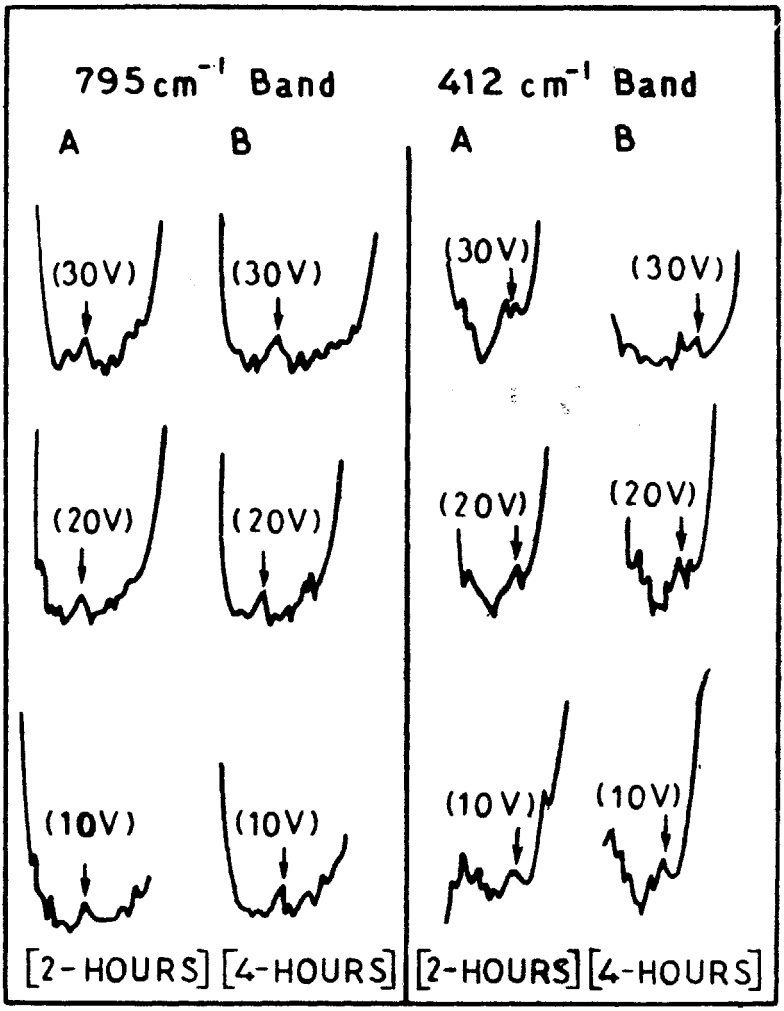

FIG 10 Growth of 795cm^{-1} and 412cm^{-1} bands with electrolysis time near cathode.

(*ii*) With increasing temp. (from 300 to 373 °K), unique asymmetric derivative signals appear. The symmetry is found to be broken at points P_1 and P_2 marked by arrows on the derivative curves as shown in Fig. 11(b) for $V = 0$ at 333 °K. This unique shape of the recorded derivative is explained by assuming the superposition of a narrow line shoulder, corresponding to interlayer water protons which are thermally activated in the lattice, over a broad proton resonance line corresponding to the coordinated water molecules being not effected by such temperatures. It is noted that the measured linewidth of the narrow line shoulder (ΔH_2) decreases with increasing temp. while that of broad proton resonance line (ΔH_1) remains constant 3.0 gauss. Hence, motional narrowing is associated with shoulder. This suggests that

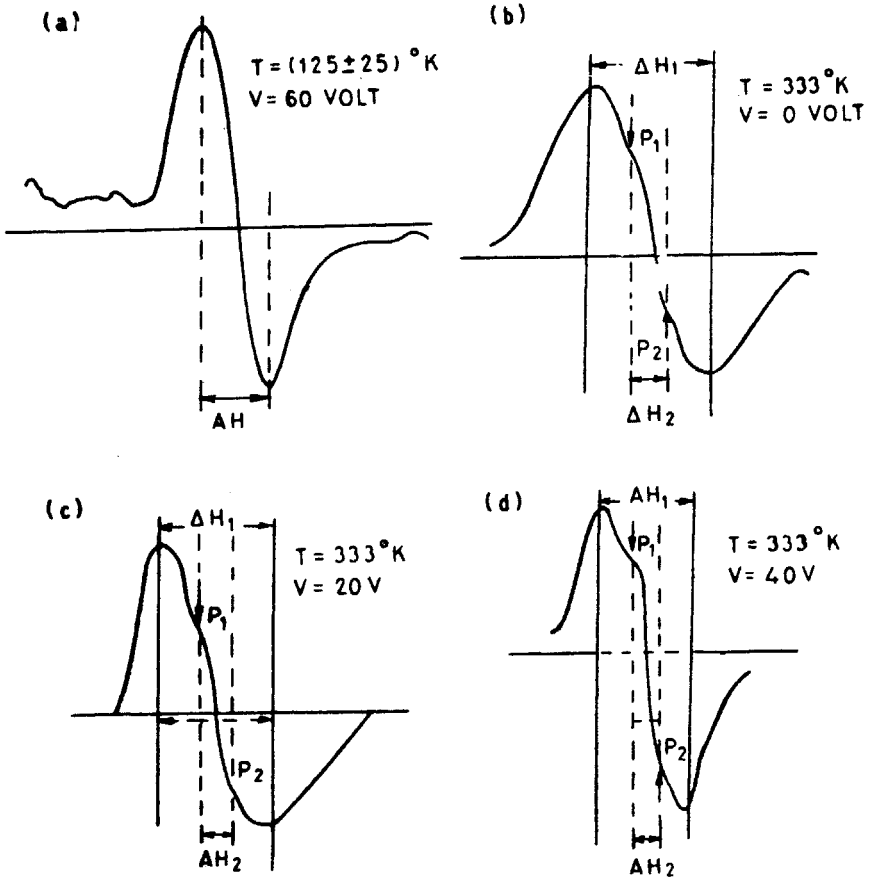

FIG 11 Recorded derivative signals corresponding to proton magnetic resonance absorption lines under different conditions.

as a thermally activated process only interlayer water protons take part in the charge transport or conductivity.

(*iii*) With increasing d.c. bias (0, 20, 40 and 60 volts) at temperatures (125 ± 25) °K, 300 °K and 333 °K proton magnetic resonance derivatives have been recorded. One such typical record is shown in Fig. 11(c and d) at 333 °K. Interestingly, the intensity of the narrow line shoulder seems to increase. The measured linewidths of the narrow line shoulder decrease with increasing d.c. bias as shown in Fig. 12. This suggests that interlayer water protons are made mobile by the applied d.c. bias. This observation suggests that studying NMR under d.c. bias can be a useful technique or experimental probe for screening possible proton conductors.

Electrical Conductivity

The detailed investigations of electrical conductivity as a function of temperature and frequency are described elsewhere. Here we describe only those results on

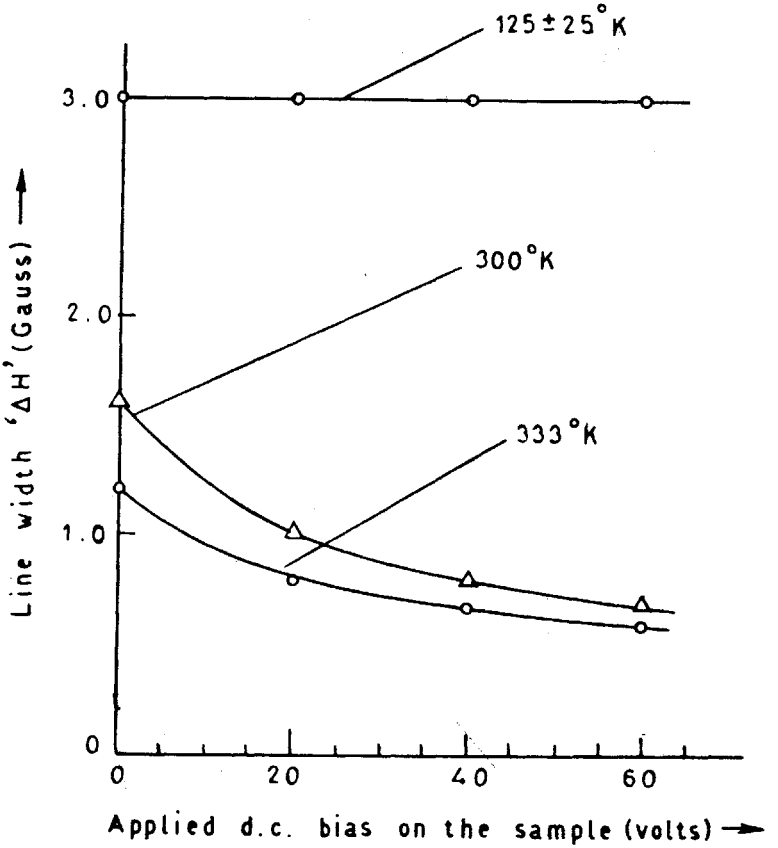

FIG 12

$MoO_3.2H_2O$ which are relevant to illustrate our point of view that possible electrolysis of water of crystallization has a role to play in electrical conductivity. If electrolysis is taking place, the number of charged ionic species would increase with d.c. bias and hence conductivity must increase accordingly. This is found to be true from the experimental results given in Table III.

TABLE III

A. C. conductivity of $MoO_3.2H_2O$ at different D.C. bias[45]

D.C. Bias in volts	100Hz (ohm^{-1} cm^{-1})	100kHz (ohm^{-1} cm^{-1})
0	2.3×10^{-6}	1.5×10^{-5}
0.5	4.7×10^{-6}	2.2×10^{-5}
1.0	6.9×10^{-6}	2.2×10^{-5}
2.0	3.6×10^{-6}	4.1×10^{-5}

Time dependence of a.c. conductivity has also been investigated. A typical result is shown in Fig. 13. The sample was first kept in vacuum. It is found that the conductivity decreases with time partly because of (*i*) polarisation and (*ii*) depletion of interlayar water of crystallization as a result of electrolysis. After this, we opened the sample to ambient atmosphere when its humidity is expected to supply the lost interlayer water molecules. As a result, we would expect the recovery of the conductivity as shown by region BC in Fig. 13. As a further consequence, the humidity of

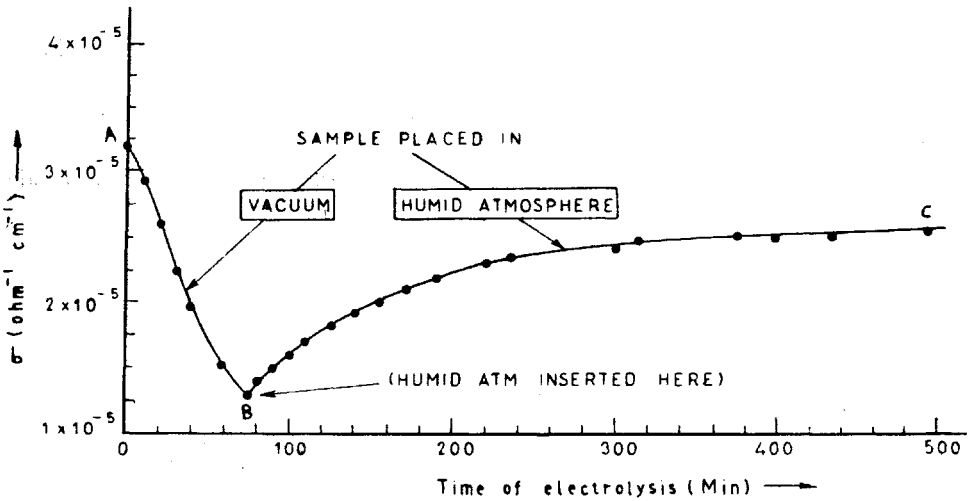

FIG 13 Time dependence of a.c. conductivity when the sample was kept in vacuum and subsequently in ambient humid atmosphere.

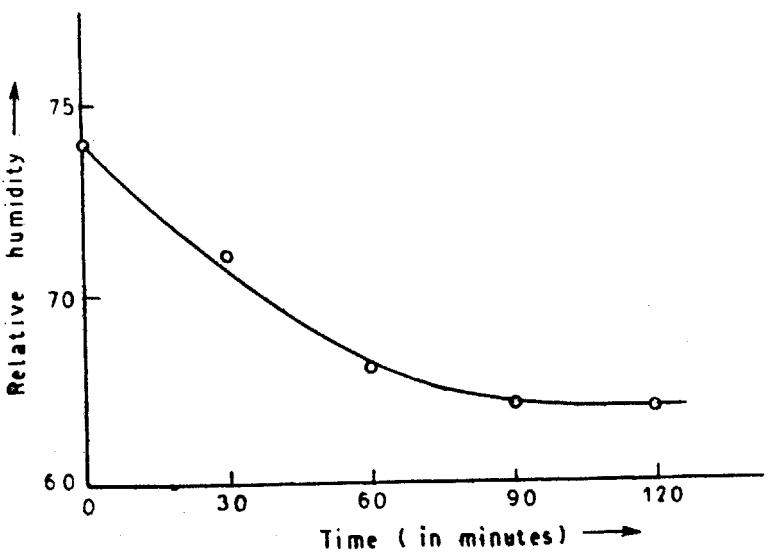

FIG 14 Variation in relative humidity with time.

the ambient would decrease. This has led us[46] to develop a device called solid state dehumidifier.

APPLICATIONS

(*i*) *Solid State De-Humidifier*

This works on the principle described earlier according to which a part of interlayer water of crystallisation of solid hydrates can be electrolysed and this loss of water of crystallisation is compensated by diffusion of water molecules from the atmosphere which subsequently leads to dehumidification. The device should be designed such that the end electrodes are able to discharge the electrolysed gaseous products H_2 and O_2 as well as the diffusion of water vapour from outside must be permitted. Pressed pellets of $MoO_3.2H_2O$ nearly 2mm thick were used to which a metallic grid (or porous platinum electrode) was attached to act as porous electrode.

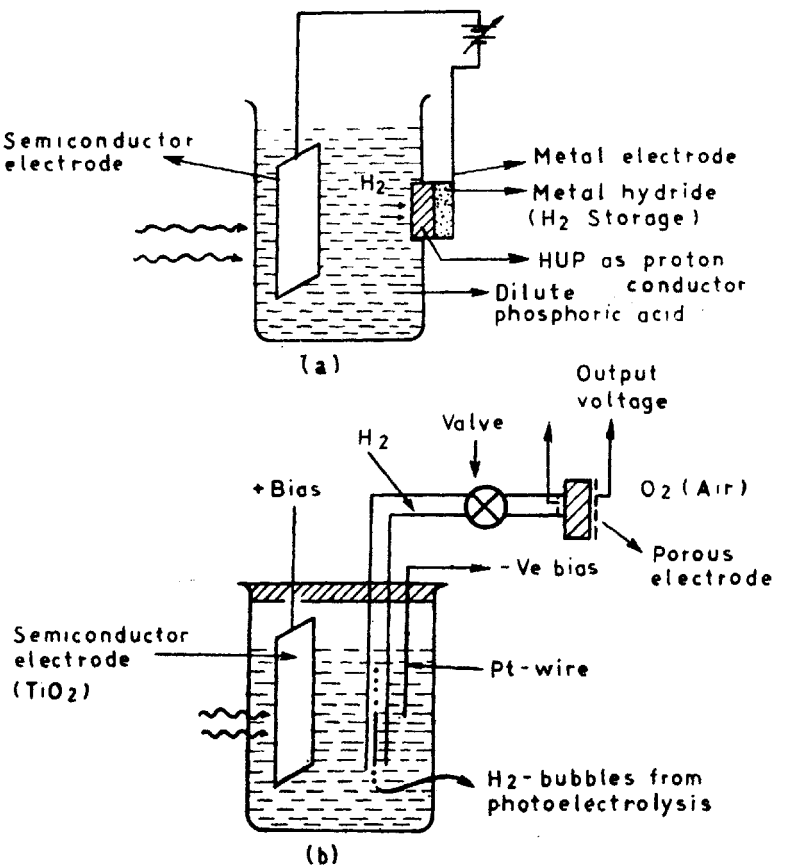

FIG 15 (*a*) Metal hydride storage of hydrogen produced by photoelectrolysis in PEC (*b*) Photoelectrolysis cell integrated with proton fuel cell for *in-situ* storage of solar energy.

On application of a small voltage, we found that humidity of the closed enclosure decreased. A typical result is shown in Fig 14.

(*ii*) *Electrochemical Devices*

(*a*) Fuel cell

(*b*) Proton battery

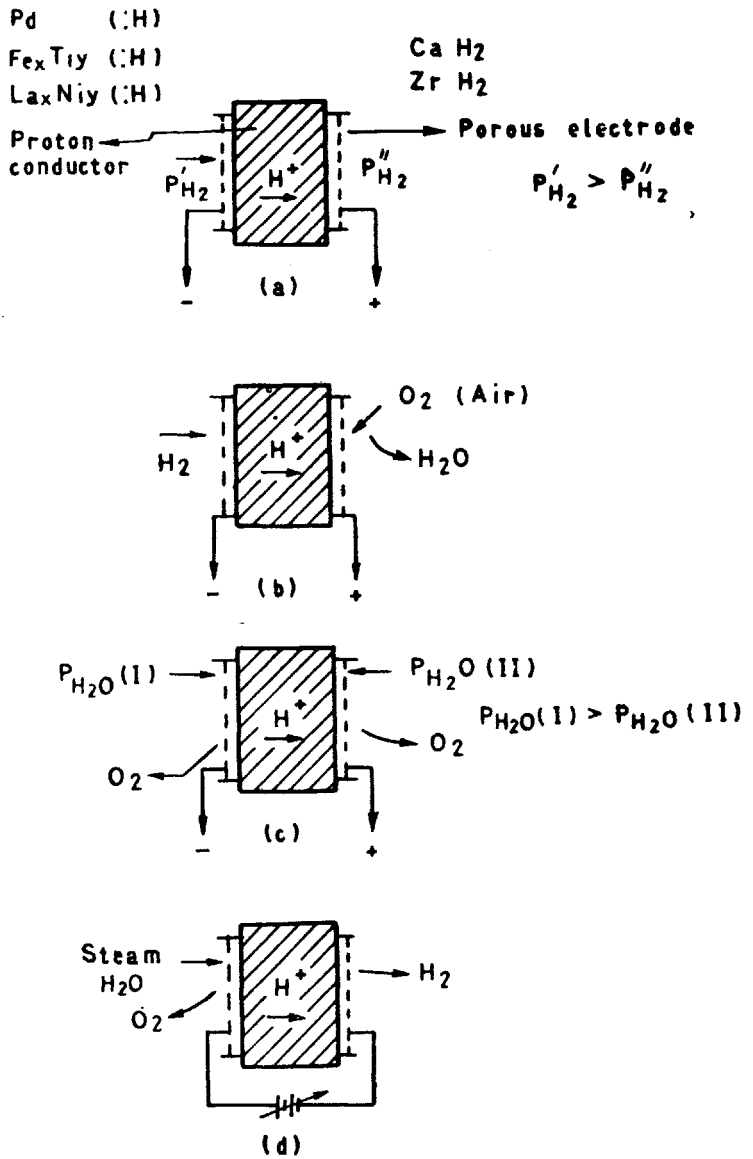

FIG 16 (*a*) Solid state proton battery (*b*) H_2-air fuel cell (*c*) humidity sensor (*d*) steam electrolysis cell.

(*c*) Gas and humidity sensors

(*d*) Steam electrolysis

The principle of the electrochemical device is simple. If the electrochemical activity of the mobile species on the two sides (a_I, a_{II}) of the proton conductors are different, a voltage is developed given by

$$E = \frac{RT}{ZF} \ln \frac{a_I}{a_{II}},$$

where F is Faraday's number and Z is the effective charge on the mobile ion. The activity difference can be created by using different gases on the two sides (H_2/O_2 in fuel cell) or the same gas at different pressures (solid state battery).

Fig. 15 shows schematically these devices. The measurement of electrochemical E.M.F. can also be used to measure the gas pressure (H_2, H_2O, etc.) on one side of the proton conductor provided the gas pressure or activity at the other end is known. Schematically gas sensors (used as humidity sensors) based on this principle are shown in Fig. 15(*c*). A novel use of proton conduction is in steam electrolysis. Suppose the proton conductor is biased as in Fig. 15(*d*). The following cell reaction results in the electrolysis:—

Anode: $H_2O(gas) \rightarrow 2H^+(electrolyte) + 1/2O_2(gas) + 2e^-(electrode)$

Cathode: $2H^+(electrolyte) + 2e^-(electrode) \rightarrow H_2(gas)$

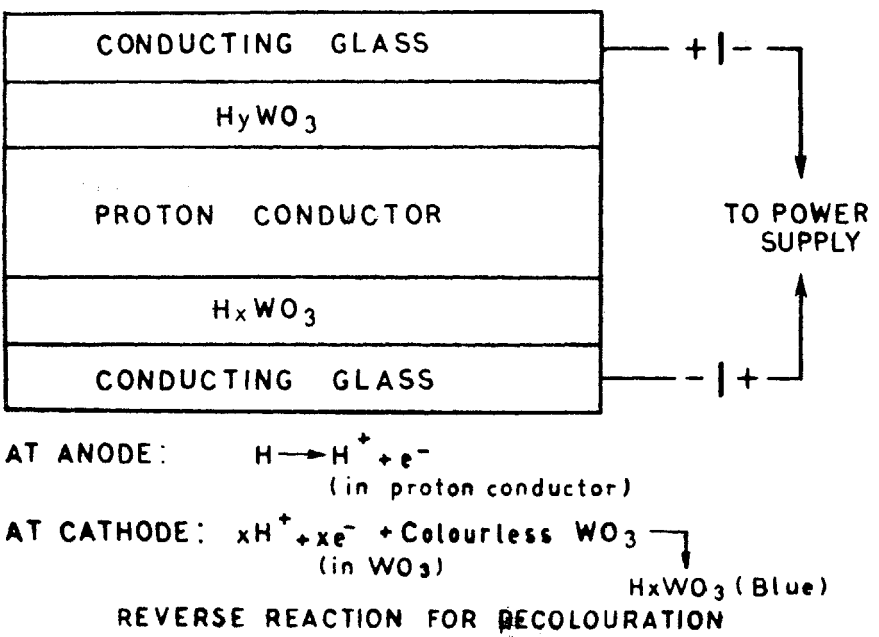

FIG 17 Schematic diagram of an electro-chromic display device.

The pure hydrogen without water vapour can be taken from the cathode compartment.

(iii) Solar Energy Storage

Recently, Schoonman,[47] Chandra and Khare *(to be published)*[48] have integrated the proton conductors into semiconductor-liquid junction photoelectrolysis cell for solar energy storage. The charge transfer between photogenerated electron-hole pairs and the aqueous electrolyte as the semiconductor electrolyte interface results in photoelectrolysis of water and the hydrogen is produced at the metal counter-electrode. In Fig. 16(*a*) the hydrogen is transported through proton conductor (HUP) and stored in a metal hydride. In Fig 16(*b*), the hydrogen produced is collected on one side of the proton conductor to be used in the H_2/air fuel cell.

(iv) Electrochromic Display Device

Fig. 17 illustrates the use of proton conductor in an electrochromic display device. A thin film of colourless WO_3 is coated on the proton conductor.

The device is biased in such a way that hydrogen is transported through the proton conductor which in turn forms a blue brozne H_xWO_3 to give the display. If the bias is reversed, the hydrogen is withdrawn from H_xWO_3 again to give a decoloured WO_3.

REFERENCES

1. S Chandra *Superionic Solids Principles and Applications* North Holland Amsterdam (1981)
2. L Glasser *Chem Rev* **75** (1975) 21
3. A B Lidiard In : *Hand Buch Phys* (*Ed* S Flugge) Springer-Varlag, Berlin **20** (1957) 246
4. S Chandra and J Rolfe Canad *J Phys* **48** (1970*a*) 397, 412
5. R G Fuller In : *Point Defects in Solids* (*Ed* J H Crawford and L M Slifkin) Plenum Press **1** (1972)
6. R J Friauf In : *Physics of Electrolytes* (*Ed* J Hladik) Academic Press **1** (1972)
7. R W Bonne and J Schoonman *J electrochem Soc* **124** (1977) 28
8. B Dunn and G C Farrington *Mater Res Bull* **15** (1980) 1773
9. W L Roth F Reidinger and A La Placa In : *Superionic Conductor Colloguium* (*Ed* G D Mohan and W L Roth) Schenectedy (1976) p 223
10. J M Reau and J Portier In : *Solid Electrolytes Fluorine Ion Conductors* (*Ed* P Hagenmuller and W van Gool) Academic Press (1978) ch 19
11. C O Tiller A C Lilly and B C Laroy *Phys Rev* **B10**(8) (1973) 4787
12. J M Reau J Portier A Levasseur G Villencuve and M Pouchard *Mater Res Bull* **13** (1978) 1415
13. J M Reau J Moali and P Hagenmuller *J Phys Chem Solids* **38** (1977) 1395
14. H Y P Hong *Mater Res Bull* **13** (1978) 117
15. F A Cotton and G Wilkinson *Inorganic Chemistry* 2nd Edn Interscience (1966) 894 and 1040
16. H Wiedersich and S Geller In : *The Chemistry of Extended Defects in Non-metallic Solids* (*Ed* L Eyring and M O Keeffe) North-Holland Amsterdam The Netherlands (1970)
17. S Geller and M D Lind *J chem Phys* **52** (1970) 5854
18. S Geller *Science* **176** (1972) 1016

19. S Geller and B B Owens *J Phys Chem Solids* **33** (1972) 1484
20. T Takahashi S Ikeda and O Yamamoto *J electrochem Soc* **119** (1972) 477
21. L Y Y Chan and S Geller *J Solid State Chem* **28** (1978) 85
22. T Forland and J Krogh-Moe *Acta Chem Scand* **11** (1957) 565
23. H Vollenkle A Wittman and H Nowatny *Mh Chem* **99** (1968) 1360
24. J T Kummer *Progr Solid State Chem Commun* **7** (1972) 141
25. F W Poulsen *Riso* **M-2244** (1980) 23
26. S H Sheffield and A T Howe *Mater Res Bull* **14** (1979) 929
27. A T Howe and M G Shilton *J Solid State Chem* **34** (1980) 149
28. O Nakamura T Kodama I Ogino and Y Miyake *Chem Lett* **17** (1979)
29. Y Wing M Lal and A T Howe *Mater Res Bull* **15** (1980) 1649
30. M G Shilton and A T Howe In : *Fast Ion Transport in Solids, Electrodes and Electrolytes* (*Ed* P Vashishta *et al.*) The Netherlands (1979)
31. G C Farrington and J L Briant *Mater Res Bull* **13** (1978) 763
32. M Lal and A T Howe *J chem Soc Chem Commun* (1980) 737
33. K D Kreuer A Rabenau and W Weppner *Angew Chem int Edn* (Engl) **21** (1982*a*) 208
34. K D Kreuer W Weppner and A Rabenau *Solid State Ionics* **314** (1981) 353
35. G C Farrington and J L Briant In: *Fast Ion Transport in Solids, Electrodes and Electrolytes* (*Ed* P Vashishta *et al.*) North Holland Amsterdam (1971)
36. K D Kreuer W Weppner and A Rabenau *Mater Res Bull* **17**(4) (1982*b*) 501
37. K D Kreuer I Stoll and A Rabenau *Solid State Ionics* **9/10** (1983) 1061
38. S Chandra and N Singh *J Phys C* **16** (1983*a*) 308
39. S K Tolpadi S Chandra S A Hashmi *Solid State Ionics* **18 & 19** (1986) 1008–1012
39*a*. S Chandra *Photoelectrochemical Solar Cells* Gordon and Breach, New York (1985)
39*b*. S Chandra In : *Transport-structure Relations in Fast Ion and Mixed Conductors* (*Ed* F W Poulsen *et al.*) 6th Riso International Symposium on Metallurgy and Materials Science (1985)
40. S Chandra and N Singh *J Phys C* **16** (1983*b*) 3099
41. J R Gunter *J Solid State Chem* **5** (1972) 354–359
42. S Srinivasan *Thesis* University of Kerala, Trivandrum, India (1979)
43. S S Saleem and G Aruldhas *Pramana* **21** (4) (1983) 283–291
44. S Chandra B Singh and N Singh *Solid State Ionics* **18 & 19** (1986) 1095–1099
45. S Chandra B Singh and N Singh *Solid State Commun* **57** (1986) 519
46. S Chandra and H D Gujrati *Indian Pat Appl* No. 1022/DEL/1985 (04/12/1985)
47. J Schoonman *Ber Bunsenges Phys Chem* **86** (1982) 660
48. S Chandra and N Khare (*Communicated*)